Chapter 9. Dielectrics, inhomogeneous materials, and plasmonics. (05 Nov 2020).



## A. Overview.

In 1904 Maxwell Garnett published a landmark paper in which he showed that the deep red color of cathedral windows containing dispersed Au nanoparticles could be explained by classical electrodynamics as a result of the interface ("screening") charge that developed when the electric field of a transmitted plane wave interacted with the nanoparticles. This is an example of plasmonics in action. This statement uses current terminology; although the technology of metal nanoparticles dispersed in glass goes back at least to the Roman empire, the terms "nanoparticle" and "plasmonics" hadn't yet been invented in 1904.

Maxwell Garnett's publication was the first paper to deal with the dielectric properties of nanoscopically inhomogeneous materials, materials that are now known as metamaterials. It is arguably also the first paper on plasmonics. Garnett showed that the color resulted from a resonance of the field-induced screening charge at the boundaries between the Au nanoparticles and the glass in which they were embedded, combined with shielding of the interior of the particles by the charge. This interpretation was particularly significant because it showed that optical properties were a function of structure as well as material. This meant that optical measurements could be used to determine structure. This capability is critical in present-day integrated-circuits technology, where optical measurements are essential for quantifying film thicknesses and subwavelength features that result from deposition, lithography, and etching.

As shown in Ch. 7, screening charge develops at any interface between two materials with different dielectric functions as a natural consequence of their different polarizabilities. It is therefore a factor in any composite material, for example the cathedral windows of the above paragraph, and nearly all deposited thin films. It is usually induced by an externally applied field, but can also exist as a free-standing excitation, i.e., a plasmon of the configuration. The former and latter cases are described mathematically as solutions of inhomogeneous and homogeneous equations, respectively. Although solutions of homogeneous equations are rarely if ever discussed in classical E&M, anyone who has ever worked with differential equations is well familiar with them, because they are needed to satisfy initial conditions.

The approach used to describe composite materials in electrodynamics depends on the ratio of the characteristic dimensions of the inhomogeneities, or domains, to the wavelength of the electromagnetic field with which they are interacting. In electrostatics

the speed of light *c*, and therefore the wavelength $\lambda$, is infinite, so in electrostatics domains of any size can be analyzed. For finite wavelengths, electrostatics remains a good approximation if the characteristic dimensions of the domains are small enough so the phase difference across any given domain is negligible. In practice this means that the size of any given domain is substantially smaller than $\lambda$ in the medium. As the characteristic-size/wavelength ratio increases, treatments go beyond electrostatics to scattering theory, and eventually to geometric optics. In Ch. 8 we assume throughout that electrostatics applies, but that any given domain is large enough to possess its own dielectric identity $\varepsilon$.

Interest in inhomogeneous materials or more generally plasmonics has peaked at least 4 times since Garnett's work: the 1935 paper of Bruggeman, which laid the foundation of optical analysis of composites; studies of surface plasmons in the late 1960's, mainly by Abelès; the discovery and application of surface-enhanced Raman scattering in the 1980's; and Pendry's mistaken claim of subwavelength imaging in 2000. Unfortunately, the relevant material has not made it into textbooks. Negative-index materials and metamaterials are newer related topics, but since these depend on permeability as well as permittivity, they wait until after we have discussed magnetic phenomena.

The treatment in Ch. 9 involves materials in general, not just conductors as in earlier chapters. Basic equations are given in Sec. B, followed in Sec. C by solutions of various boundary-value problems involving dielectrics. Section C also covers plasmonic solutions of these configurations. In Sec. D the results of Sec. C are used to develop various effective-medium approximations (EMAs), which are models that provide analytic descriptions of the dielectric responses of composite materials to which the electrostatics approximation applies. Limit theorems, which put surprisingly restrictive boundaries on allowed values of $\varepsilon$ even if nothing is known about the nanostructure of the material, are discussed in Sec. E. Additional aspects of plasmons are covered in Sec. F.

## B. Basic equations.

The macroscopic equations pertaining to boundary-value problems are developed in Ch. 7. These are

$$\vec{D} = \varepsilon \vec{E} = \vec{E} + 4\pi \vec{P}\,; \tag{9.1a,b}$$

$$\nabla \cdot \vec{D} = 4\pi \rho_o\,; \tag{9.1c}$$

$$\nabla \cdot \vec{E} = 4\pi\rho_o + 4\pi\rho_P = 4\pi\rho_o - 4\pi \nabla \cdot \vec{P}\,; \tag{9.1d,e}$$

where

$$-\nabla \cdot \vec{P} = \rho_P \tag{9.1f}$$

is the polarization charge density that describes the response of the system to the applied electric field. For uniform materials $-\nabla \cdot \vec{P} = 0$ in the bulk, but by applying a Gauss' Theorem to a Gaussian pillbox straddling an interface (see diagram on next page), we find that

$$\vec{n}\cdot(\vec{E}_2-\vec{E}_1)=4\pi\sigma_P\,, \tag{9.2}$$

or $-\nabla\cdot\vec{P}=\sigma_P\delta(z)$ to a good approximation. The polarization surface charge density $\sigma_p$ at the interface is generally termed screening charge because of its role in reducing ("screening") fields inside materials relative to fields outside if the "inside" dielectric function is the greater of the two.

If $\rho_o=0$, then Gauss' Theorem applied to Eq. (9.1c) yields

$$\hat{n}\cdot(\vec{D}_2-\vec{D}_1)=0\,, \tag{9.3}$$

where $\hat{n}$ is the unit surface normal vector pointing in the direction of $\vec{D}_2$. Thus the normal component of $\vec{D}$ is continuous at an interface whether or not a screening charge is developed. Thus Eq. (9.3) is a constraint, which when applied allows electrostatics problems with boundaries between materials with different dielectric functions to be solved conveniently. Equation (9.2) is not a constraint, but only a recipe for calculating $\sigma_P$.

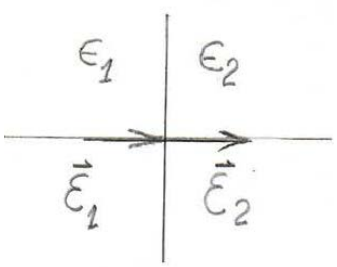


The remaining continuity condition follows from

$$\nabla\times\vec{E}=0\,, \tag{9.4}$$

which with Stokes' Theorem shows that the transverse component of $\vec{E}=-\nabla\phi$ is continuous at an interface. If $\phi$ is continuous across an interface, then the tangential component of $\nabla\phi$ will also be continuous. Applying the continuity condition to $\phi$ instead of the tangential component of $\nabla\phi$ results in a significant saving of effort.

Background material for $\sigma_P$ appears in Ch. 8, and for conductors, in Ch. 7. For a conductor under static conditions, screening is perfect: $\sigma_P$ ensures that an external field does not penetrate into a conductor. At finite frequencies screening is imperfect and internal fields occur. While internal fields generally follow directly from applied fields, another class involves solutions of the homogeneous equations. These are the elementary excitations of the configuration, i.e., plasmons. These exist only at specific values of $\varepsilon$, hence at particular frequencies $\omega$ that are characteristic of the configuration.

C. Boundary-value problems with dielectrics.

This section consists entirely of examples, in part to establish the foundation for developing effective-medium theory and understanding plasmonics. "Dielectric" is taken to mean any material, including metals. It is only necessary that the material has a dielectric function $\varepsilon$.

*Sheet of dielectric material of dielectric function $\varepsilon$ and thickness d in empty space.* Let an external field $\vec{D}_o=\vec{E}_o$ be applied at normal incidence to the sheet. Then by the boundary condition on normal $\vec{D}$, the electric field inside the sheet is

$$\vec{E}_{in} = \frac{\vec{D}_o}{\varepsilon} = \frac{\vec{E}_o}{\varepsilon}. \tag{9.5}$$

This agrees with our intuition, which suggests that for $\varepsilon > 1$, the magnitude of the field in the material must be lower than that of the outside field that created it. The interface charge density on the side where $\vec{E}_o$ points away from the slab is therefore

$$\sigma_P = \frac{1}{4\pi}(E_o - E_{in}) = \frac{1}{4\pi}\left(1 - \frac{1}{\varepsilon}\right)E_o. \tag{9.6}$$

Plasmons: Suppose that $E_o$ and $\varepsilon$ are both zero. Then Eq. (9.5) becomes

$$\vec{E}_{in} = \frac{0}{0}. \tag{9.7}$$

Because $0/0$ is indeterminate, Eq. (9.7) shows that for $\varepsilon = 0$ a field can exist in the material even if no external field is present. The condition $\varepsilon = 0$ is realized in principle with a Drude metal at $\omega = \omega_p$. This explains in part why $\omega_p$ is called the plasma frequency. The plasmon requires input energy to get the resonance started, although once started it can exist indefinitely if there is no loss. The resonance represents the cyclic transfer of energy at $\omega = \omega_p$ between the magnetic field created by current flow and the electric field created by separation of charge. These plasmonic solutions are only stable dynamically.

The three-dimensional analog of the above one-dimensional solution also exists. Consider a positive point charge *q* injected into a metal. Electrons respond by rushing in to screen *q*, overshoot, rebound, overshoot again, etc., at the frequency $\omega_p$. The single dimension in this case is the radial coordinate *r*. These bulk-plasmon oscillations typically exhibit considerable loss and tend to damp out rapidly.

*Dielectric sphere in a uniform external field.* This is the classic boundary-value problem in electrostatics. Let the radius of the sphere be *a*, its dielectric function be $\varepsilon$, the ambient dielectric function be $\varepsilon_a = 1$, and the applied field be $\vec{E} = E_o\hat{z}$, as indicated schematically in the figure. $E_o\hat{z}$ polarizes the sphere, generating an internal field that is a scaled version of the applied field, and an external field of a dipole. The dipole in fact is perfect: we find below that no higher multipole moments exist. If the sphere is a conductor, then under static conditions the internal field is zero, i.e., the screening is perfect. One might consider this the first example of cloaking.

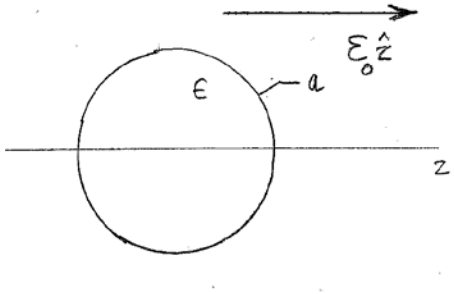


Taking advantage of symmetry, the trial solutions for the interior and exterior potentials are

$$\phi_{in}(r,\theta,\varphi) = \sum_{l=0}^{\infty} A_l \left(\frac{r}{a}\right)^l P_l(\cos\theta)\,; \tag{9.8a}$$

$$\phi_{out}(r,\theta,\varphi) = -E_o z + \sum_{l=0}^{\infty} B_l \left(\frac{a}{r}\right)^{l+1} P_l(\cos\theta)\,. \tag{9.8b}$$

We separate appropriate powers of the radius *a* from $A_l$ and $B_l$ to simplify the math. The continuity condition on $\phi$ at $r = a$ is

$$\sum_{l=0}^{\infty} A_l P_l(\cos\theta) = -E_o a\cos\theta + \sum_{l=0}^{\infty} B_l P_l(\cos\theta)\,. \tag{9.9a}$$

The continuity condition on normal $\vec{D}$ is

$$(-l\varepsilon)\sum_{l=0}^{\infty} A_l \left(\frac{1}{a}\right) P_l(\cos\theta) = E_o\cos\theta - (-l-1)\sum_{l=0}^{\infty} B_l \left(\frac{1}{a}\right) P_l(\cos\theta)\,. \tag{9.9b}$$

Since the source term is $z = r\cos\theta = rP_1(\cos\theta)$, only the $l = 1$ term survives. Then

$$A_1 - B_1 = -aE_o\,; \tag{9.10a}$$

$$\varepsilon A_1 + 2B_1 = -aE_o\,. \tag{9.10b}$$

Therefore,

$$\phi_{in}(r,\theta,\varphi) = -\frac{3}{\varepsilon+2} E_o z\,; \tag{9.11a}$$

$$\varphi_{out}(r,\theta,\phi) = -E_o z + \left(\frac{\varepsilon-1}{\varepsilon+2}\right)\left(\frac{a^2}{r^2}\right) aE_o\cos\theta\,. \tag{9.11b}$$

The result is reasonable: when $\varepsilon = 1$, the field inside the sphere is the applied field, and the second term in Eq. (9.11b) vanishes. When $\varepsilon \to \infty$, $\phi_{in} = 0$, corresponding to the complete screening encountered with a metal.

The exterior potential due to the sphere is that of a dipole of strength

$$p = \frac{\varepsilon-1}{\varepsilon+2} a^3 E_o\,. \tag{9.12}$$

The absence of multipole moments $l \neq 1$ means that this is a *perfect* dipole, in contrast to a pair of charges $\pm q$ separated by a small distance *d*.

We next consider the screening charge. The calculation is straightforward. We find

$$\hat{r}\cdot(\vec{E}_{out} - \vec{E}_{in})\Big|_{r=a} = 4\pi\sigma_s = 3E_o\left(\frac{\varepsilon-1}{\varepsilon+2}\right)\cos\theta\,. \tag{9.13}$$

This is qualitatively what we expect for the sphere in an external field: if $\varepsilon > 1$ then $\sigma_s$ is positive in the field direction, negative in the opposite direction, and vanishes on the bisector orthogonal to the field.

Equations (9.14) have a pole at $\varepsilon = -2$, which we now recognize as the signature of the solution of the homogeneous equation. However, with no external drive field $E_o\hat{z}$ to break the spherical symmetry, more general solutions are possible. These are

$$\phi_{in}(r,\theta,\varphi) = \sum_{l=0}^{\infty}\sum_{m=-l}^{l} A_{lm}\left(\frac{r}{a}\right)^{l} Y_{lm}(\theta,\varphi)\,; \tag{9.14a}$$

$$\phi_{out}(r,\theta,\varphi) = \sum_{l=0}^{\infty}\sum_{m=-l}^{l} B_{lm}\left(\frac{a}{r}\right)^{l+1} Y_{lm}(\theta,\varphi)\,; \tag{9.14b}$$

At $r = a$, the continuity condition on $\phi$ yields

$$A_{lm} = B_{lm}\,, \tag{9.15a}$$

while that on normal $\vec{D}$ yields

$$\varepsilon l A_{lm} = -(l+1) B_{lm}\,. \tag{9.15b}$$

Given that $A_{lm} = B_{lm}$, Eqs. (9.14) have a nontrivial solution if

$$\varepsilon = -1 - 1/l\,. \tag{9.16}$$

This is independent of *m*, and reduces to the prior case of $\varepsilon = -2$ for $l = 1$.

Thus the sphere has a countably infinite number of plasmons. This is reasonable, for with no symmetry constraints, all the $Y_{lm}(\theta,\varphi)$ are equally valid. Thus the sphere can support dipole, quadrupole, octupole, etc. plasmons, each of which has a different resonance frequency.

*Point charge adjacent to a dielectric plane: method of images.* This configuration consists of a point charge *q* located a distance *d* away from a dielectric of dielectric function $\varepsilon$ that fills all space $z < 0$, as indicated in the diagram. This is a generalization of the same configuration that we examined in Ch. 8 for a conductor. The difference now is that the field is no longer perpendicular to the interface at $z = 0$, so mirror symmetry won't work. A more general approach is needed.

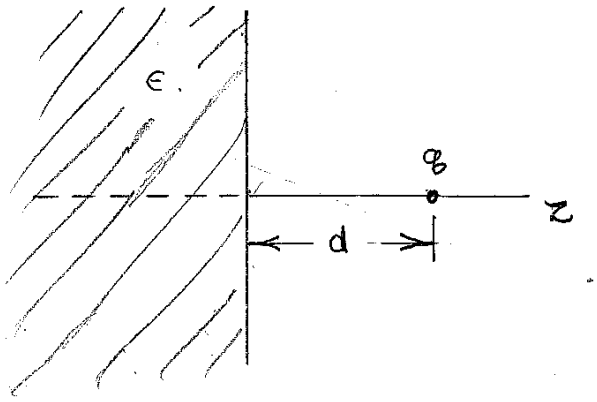


However, this problem can still be solved using the image-charge method. Start by deciding on the number of image charges and their locations. Because the boundary conditions require that the scalar potential and of the normal component of $\vec{D}$ be continuous everywhere at $z = 0$, we can anticipate that two degrees of freedom are needed. These would be two virtual charges $q'$ and $q''$, one from the air side and the other on the material side. Thus on the air side

$$\phi_a(\vec{r}) = \frac{q}{\sqrt{x^2 + y^2 + (z-d)^2}} + \frac{q'}{\sqrt{x^2 + y^2 + (z+d)^2}}. \tag{9.17}$$

The virtual charge $q'$ must obviously be the same distance *d* from the interface as *q* to ensure that the two denominators are equal for all $\rho$ at $z = 0$.

The same denominator argument also works on the dielectric side. Because $q''$ is a virtual charge, it therefore superposes on *q*. This is consistent with the microscopic model, where $\sigma_P$ is viewed as a charge sheet in its own right, and is symmetric about $z = 0$. Then for $z > 0$,

$$\phi_d(\vec{r}) = \frac{q''}{\sqrt{x^2 + y^2 + (z-d)^2}}. \tag{9.18}$$

Symmetry also implies that $q'$ and $(q - q'')$ must be equal. However, rather than treat this as a condition, we follow the usual strategy of applying the boundary conditions on $\phi$ and the normal component of $\vec{D}$, then verify this relation at the end.

At $z = 0$ the boundary condition on $\phi$ is

$$q + q' = q''. \tag{9.19a}$$

and that on normal $\vec{D}$ is

$$-qd + q'd = -\varepsilon q''d\ . \tag{9.19b}$$

The solution is

$$q' = -q\frac{\varepsilon - 1}{\varepsilon + 1}; \quad q'' = q\frac{2}{\varepsilon + 1}. \tag{9.20a,b}$$

These expressions reduce properly to $q' = 0$ and $q'' = q$ when $\varepsilon = 1$, and also $q' = -q$ and $q'' = 0$ when $\varepsilon \to \infty$. Also, $q - q' = -q''$ as expected by symmetry.

The solutions diverge for $\varepsilon = -1$. This is the $k = 0$ interface plasmon, which is discussed in Sec. F and will appear again when we treat reflection.

D. Composite materials: effective-medium theories.

The goal of effective-medium theory is to develop methods of describing the dielectric response of a composite material with a dielectric function that can be used in the same way as those of materials that are uniform on a macroscopic scale. A composite material is defined as a mixture of two or more materials of regions of dimensions small compared to the wavelength of light but large enough so that each is described by its own dielectric function. The procedure used to determine the composite dielectric response of these materials is identical to that which we used for uniform materials in Ch. 7, except the regions are now described by specific sizes, shapes, and dielectric functions. The new physics – and the challenge – is to deal with the screening charge that develops between regions.

The dielectric function of the composite is defined according to the usual expression $<\vec{D}>=<\varepsilon><\vec{E}>$, except that $W(\vec{r}-\vec{r}')$ no longer averages over dipoles but over internal fields where the dielectric response is a piecewise-constant function of $\vec{r}'$. In the notation of Ch. 8, the averages of $\vec{D}$ and $\vec{E}$ are

$$<\vec{D}>=\frac{1}{V}\int_V d^3r' W(\vec{r}-\vec{r}')\,\varepsilon(\vec{r}')\vec{E}(\vec{r}'), \tag{9.21a}$$

$$<\vec{E}>=\frac{1}{V}\int_V d^3r' W(\vec{r}-\vec{r}')\vec{E}(\vec{r}'), \tag{9.21b}$$

where $\varepsilon(\vec{r})$ and $\vec{E}(\vec{r})$ are the dielectric function and electric field at a given point $\vec{r}$ in the composite, and $V$ is its overall volume. In simple cases $\varepsilon$ can be represented analytically. Specific solutions of this type are termed *effective medium approximations* (EMAs). EMAs are significant not only for convenience but also, as noted above, because they extend optical-diagnostics capabilities beyond simple materials analysis into structure.

*Cermet microstructures: Maxwell Garnett effective-medium approximation*. The basic configuration is shown in the diagram. It consists of spheres of radius *a* and dielectric function $\varepsilon_b$ embedded in an extended "host" medium of dielectric function $\varepsilon_a$. This is the *cermet* nanostructure, where every inclusion is completely surrounded by the host medium and the inclusions are relatively far apart. If the spheres are more polarizable than the medium in which they are embedded, as is usually the case, application of an initially uniform external field causes the development of screening charge of the polarity shown in the figure. The Garnett EMA is a starting point for more elaborate EMAs. These include not only geometries where the inclusions are nonspherical, but also for *aggregate* configurations, where the different regions are randomly mixed and there is no clear distinction between host and inclusion. Aggregates will be discussed below.

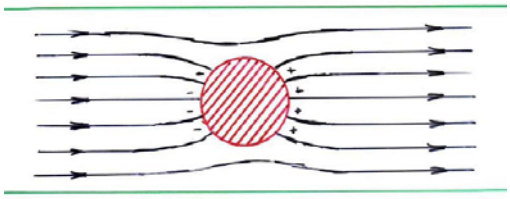

To derive the Garnett EMA, assume that a large region of volume $V$ contains a small spherical inclusion of volume $V_b=(4/3)\pi a^3$ at its center. The dielectric functions of the host material and the inclusion are $\varepsilon_a$ and $\varepsilon_b$, respectively. To do the calculation, a field $\vec{E}=E_o\hat{z}$ is applied. The dielectric function $\varepsilon$ of the composite is calculated by first obtaining $\vec{E}(\vec{r})$ and $\vec{D}(\vec{r})$, then applying Eqs. (9.21). The difference between this calculation and similar calculations in Ch. 8 is that the inclusions are not point dipoles but have a finite volume. Generalizing Eqs. (9.14) to a host medium of dielectric function $\varepsilon_a\neq 1$ gives

$$\vec{E}_{in}(\vec{r})=\sum_{\vec{R}_n}\hat{z}E_o\frac{3\varepsilon_a}{\varepsilon_b+2\varepsilon_a}u(a-|\vec{r}-\vec{R}_n|) \tag{9.22a}$$

for the field in each inclusion, and

$$\vec{E}_{host} = \sum_{\vec{R}_n} \left[ \hat{z}E_o + \frac{3((\vec{r}-\vec{R}_n)\cdot\vec{p})(\vec{r}-\vec{R}_n) - (\vec{r}-\vec{R}_n)^2\,\vec{p}}{|\vec{r}-\vec{R}_n|^5} \right] \Big(1 - u(a - |\vec{r}-\vec{R}_n|)\Big), \qquad (9.22b)$$

in the host, where the spherical inclusions are described as dipoles

$$\vec{p} = \hat{z}\frac{\varepsilon_b - \varepsilon_a}{\varepsilon_b + 2\varepsilon_a} a^3 E_o \,. \qquad (9.22c)$$

The corresponding displacement fields $\vec{D}_{out}$ and $\vec{D}_{in}$ are obtained by multiplying $\vec{E}_{out}$ and $\vec{E}_{in}$ by $\varepsilon_a$ and $\varepsilon_b$, respectively.

To calculate the spatial average of Eqs. (9.22), break the complete volume integral into two parts. The interior part is

$$\int_{V_b} d^3r' W(\vec{r}-\vec{r}')\vec{E}_{in} = \int_V d^3r' W(\vec{r}-\vec{r}') \sum_{\vec{R}_n} \hat{z}E_o \frac{3\varepsilon_a}{\varepsilon_b + 2\varepsilon_a} u(a - |\vec{r}-\vec{R}_n|) \qquad (9.23a)$$

$$= \hat{z}E_o \frac{3\varepsilon_a}{\varepsilon_b + 2\varepsilon_a} \sum_{\vec{R}_n} \int_V d^3r' W(\vec{r}-\vec{r}') u(a - \vec{r} - \vec{R}_n|)| \qquad (9.23b)$$

$$= \hat{z}E_o \frac{3\varepsilon_a}{\varepsilon_b + 2\varepsilon_a} f_b \ , \qquad (9.23c)$$

where $f_b$ is the volume fraction of the inclusions. The assumption made in going from Eq. (9.23b) to Eq. (9.23c) is that the "pockets" corresponding to the inclusions have dimensions small compared to the spread of $W(\vec{r}-\vec{r}'))$ but are sufficiently numerous that the sum gives a good representation of a scaled version of $W(\vec{r}-\vec{r}'))$ in the integral over V.

Repeating the calculation for $\vec{E}_{host}$ is simpler because the volume integral of the dipole term is nonzero only if the integral accesses the dipole itself. Since the dipoles are excluded from the host region only the integration over $\hat{z}E_o$ survives. The result is

$$\int_{V_a} d^3r' W(\vec{r}-\vec{r}')\vec{E}_{host} = \hat{z}E_o(1 - f_b) = \hat{z}E_o f_a \,, \qquad (9.24)$$

where $f_a = 1 - f_b$ is the volume fraction of the host. The entire volume integral is then the sum of the two, or

$$< \vec{E} > = \left( f_a + f_b \frac{3\varepsilon_a}{\varepsilon_b + 2\varepsilon_a} \right) \vec{E}_o \,; \qquad (9.25a)$$

$$< \vec{D} > = \left( \varepsilon_a f_a + \varepsilon_b f_b \frac{3\varepsilon_a}{\varepsilon_b + 2\varepsilon_a} \right) \vec{E}_o \,. \qquad (9.25b)$$

Using the definition $<\vec{D}> = \varepsilon <\vec{E}>$, the result is

$$\varepsilon = \frac{(\varepsilon_b + 2\varepsilon_a) + 2f_b(\varepsilon_b - \varepsilon_a)}{(\varepsilon_b + 2\varepsilon_a) - f_b(\varepsilon_b - \varepsilon_a)}. \tag{9.26a}$$

Equation (8.29a) is the Garnett effective-medium approximation. It is usually written in the more symmetric form

$$\frac{\varepsilon - \varepsilon_a}{\varepsilon + 2\varepsilon_a} = f_b \frac{\varepsilon_b - \varepsilon_a}{\varepsilon_b + 2\varepsilon_a}. \tag{9.26b}$$

It can be noted that the radius *a* of the general spherical inclusion is not used. Thus Eqs. (9.26) also apply to inclusions with random radii, as long as the inclusions do not get too small to retain their dielectric identity, too large to be treated in the electrostatic approximation, or close enough together so the internal fields begin to interfere. Even when any or all of these assumptions are violated, the limit theorems discussed below show that Eqs. (9.29) remain a good approximation in most cases, even if nothing is known about the structure of the composite.

*Laminar configuration.* A laminar stack of materials of alternating dielectric functions $\varepsilon_a$ and $\varepsilon_b$ is another configuration that can be solved exactly. While it hardly represents a random mix of materials, it is important because it leads to the Wiener limits, which were derived in 1912 and specify absolute extremal values of the dielectric function of the composite for any structure and any relative volume fraction.


Consider first the case where the external field $\vec{E}_o$ is applied parallel to the laminations, as indicated in the diagram. Let the material consist of alternating layers of material *a*, with dielectric function $\varepsilon_a$, and material *b*, with dielectric function $\varepsilon_b$. Since the field is parallel to all boundaries, the relevant boundary condition is tangential $\vec{E}$ continuous, so $\vec{E}(\vec{r}) = \vec{E}_o$ throughout. Hence the average field is $<E> = \vec{E}_o$. Also, since $\vec{E}_o$ is constant throughout the volume, $\nabla \cdot \vec{E} = 0$ everywhere, so no screening charge exists at any boundary.

The local displacement field $\vec{D}(\vec{r})$ is piecewise constant, depending on whether $\vec{r}$ is in medium *a* or *b*. Thus the average displacement field is

$$<\vec{D}> = \frac{\vec{E}_o}{V}\int_V d^3r\,\varepsilon(\vec{r}) = (f_a\varepsilon_a + f_b\varepsilon_b)\vec{E}_o, \tag{9.27}$$

where $f_a$ and $f_b$ are the relative volume fractions of materials *a* and *b*, respectively, and as usual $f_a + f_b = 1$. Thus for the laminar sample with the field parallel to the laminations

$$\varepsilon = f_a\varepsilon_a + f_b\varepsilon_b. \tag{9.28}$$

This is simply the arithmetic average of the dielectric functions of the constituents, weighted by their relative volume fractions. This is what one might expect in the absence of screening charge. The electric-circuit equivalent of this configuration is capacitors in parallel.

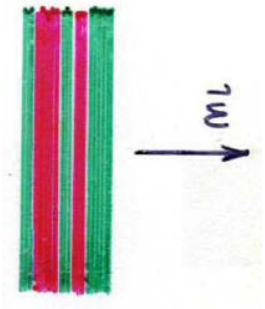


If the field is oriented perpendicular to the layers, as indicated by the diagram at the right, the relevant boundary condition is normal $\vec{D}$ continuous. If an external field $\vec{E}_o = \vec{D}_o$ is applied, a constant displacement field $\vec{D}(\vec{r}) = \vec{D}_o$ is generated throughout. Then $<\vec{D}> = \vec{D}_o$ and

$$<\vec{E}> = f_a \frac{\vec{D}_o}{\varepsilon_a} + f_b \frac{\vec{D}_o}{\varepsilon_b}. \tag{9.29}$$

In this case

$$\frac{1}{\varepsilon} = \frac{f_a}{\varepsilon_a} + \frac{f_b}{\varepsilon_b}. \tag{9.30}$$

The electric field is now discontinuous at each internal boundary, so screening charge appears. This charge is given by

$$\sigma_{ab} = -\nabla \cdot \vec{P} = \frac{1}{4\pi} \nabla \cdot \vec{E} = \frac{\vec{D}_o}{4\pi} \left( \frac{1}{\varepsilon_b} - \frac{1}{\varepsilon_a} \right) \tag{9.31}$$

crossing from region *a* to *b*. Because the internal fields are perpendicular to the planar boundaries at all points, the total amount of screening charge in the configuration is a maximum. The analogous circuit configuration is capacitors in series.

Although the laminar configuration is the same in the two situations, the results clearly depend on the direction at which the external field is applied. This configuration therefore illustrates the importance of the direction of the applied field relative to the internal boundaries of the composite in determining the effective dielectric response. In fact, it allows us to go one step further. Because there can never be less screening charge than no screening charge, nor more screening charge than the maximum, these two configurations represent absolute constraints – the Wiener limits – on values that the dielectric function of a composite material can obtain, no matter how clever one is in constructing nanostructures. We will discuss this, and and other limit theorems, in Sec. E.

*Generalizations of the Garnett EMT.* The Garnett result depends not only on the inclusion being spherical, but also that all inclusions are well removed from each other. Thus the volume fraction $f_b$ is necessarily small compared to 1. If the inclusions are close enough so that they interact, the internal fields will no longer be described by isolated dipoles, and numerical solutions are generally required.

However, the Garnett EMA can still be used as a starting point for more extended approximations. Start by changing the notation of the dielectric function of the "host"

material from $\varepsilon_a$ to $\varepsilon_h$, and suppose that there are two types of inclusions. A suitable generalization of Eq. (8.31) is then

$$\frac{\varepsilon-\varepsilon_h}{\varepsilon+2\varepsilon_h}=f_a\frac{\varepsilon_a-\varepsilon_h}{\varepsilon_a+2\varepsilon_h}+f_b\frac{\varepsilon_b-\varepsilon_h}{\varepsilon_b+2\varepsilon_h}. \tag{9.32}$$

It is clear that Eq. (9.32) reduces to Eq. (9.31) if $\varepsilon_h$ equals either $\varepsilon_a$ or $\varepsilon_b$. More terms can be added to the right side of Eq. (9.32) as necessary.

It was soon recognized that Eq. (9.26b) is not symmetric in *a* and *b*. A different value of $\varepsilon$ is obtained if *a* is embedded in *b* than if *b* is embedded in *a*. This causes problems if the volume fractions are comparable, because the question then arises as to what is embedded in what. This issue was resolved by Bruggeman, who adopted the mean-field approach of embedding both *a* and *b* in $\varepsilon$. With $\varepsilon=\varepsilon_h$ Eq. (8.32) reduces to

$$0=f_a\frac{\varepsilon_a-\varepsilon}{\varepsilon_a+2\varepsilon}+f_b\frac{\varepsilon_b-\varepsilon}{\varepsilon_b+2\varepsilon}. \tag{9.33}$$

This is the *Bruggeman effective-medium approximation.* It reduces to the Garnett EMA for dilute mixtures, but can still deal with mixtures that are closely packed and those where the grains have random shapes. These are common characteristics of evaporated thin films, where the grain boundaries between nanocrystals represent inefficient packing. The Bruggeman EMA is also used to describe the dielectric properties of surfaces that are rough on a nanoscopic scale.

An evaporated film of Au is a good example of a composite consisting of a random mixture of Au crystallites and empty space, since for a face-centered-cubic metal approximately half a monolayer of atoms is lost at each boundary. The figure shows dielectric function data of Au films evaporated on substrates at different temperatures. At the highest temperature the atoms have more mobility and can more effectively find their preferred crystallographic positions, so the grain sizes are larger than in films deposited at lower temperatures. Using Eq. (9.33) in the limit that the void fraction $f_a$ representing empty space is small, the dielectric function of the composite is that of Au scaled by

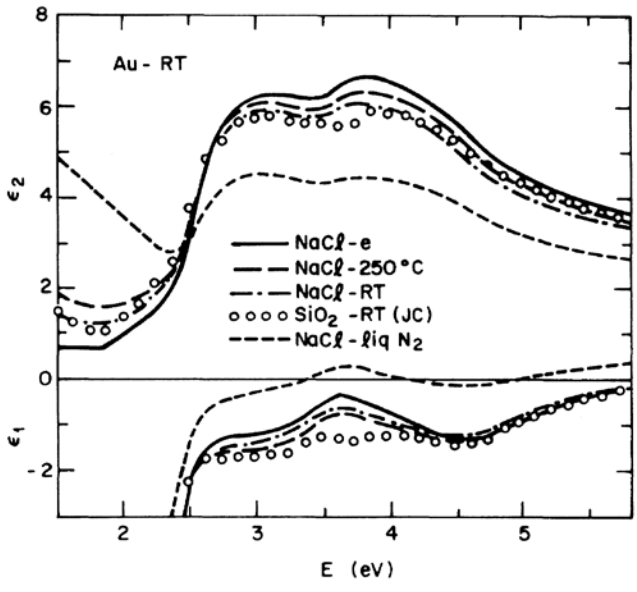


$$\eta=\left(1-\frac{3}{2}f_a\right). \tag{9.34}$$

Scaling is seen to give a good representation of the data. The tail in $\varepsilon_2$ that appears at low energies in material deposited at low temperatures is a manifestation of energy loss due to scattering of electrons at grain boundaries, which becomes dominant for small grain sizes.

The "2" that appears in the denominator of the above expressions is the depolarization factor that follows from our choice of spherical inclusions. Had we assumed two-dimensional symmetry with the inclusions taking the form of circular cylinders for an applied field perpendicular to the axes of the cylinders, then a repeat of the above derivation using functions appropriate to the Lorenzian in cylindrical coordinates would yield

$$\frac{\varepsilon - \varepsilon_a}{\varepsilon + \varepsilon_a} = f_b \frac{\varepsilon_b - \varepsilon_a}{\varepsilon_b + \varepsilon_a}. \tag{9.35}$$

More generally, we can use an arbitrary depolarization factor *p* and write

$$\frac{\varepsilon - \varepsilon_a}{\varepsilon + p\varepsilon_a} = f_b \frac{\varepsilon_b - \varepsilon_a}{\varepsilon_b + p\varepsilon_a}, \tag{9.36}$$

where $0 \le p \le \infty$. The parameter *p* is related to the more usual Lorentz depolarization factor $q_z$ by $q_z = 1/(1+p)$. This generalization includes all the expressions that we have discussed so far. For example for $p \to \infty$ we obtain Eq. (9.28), and for $p = 0$ Eq. (9.30). These correspond to the cases of no screening and maximum screening, respectively.

Of the various effective-medium approximations that have been proposed, one of the more interesting is that due to Sen, Scala, and Cohen (SSC). This was developed to describe percolation through sedimentary rocks, but also can be used in E&M. Sen et al. was an employee of Exxon, and one of the main technological challenges that Exxon faces is the extraction of petroleum from deposits in sedimentary rocks. These rocks are formed by deposition of minerals dissolved in water onto seed crystals. Because of this growth mechanism, in principle any rock contacts any other rock only at points of measure zero. No matter what the volume fraction of rock, the water is the continuous phase and therefore is the host material. The SSC model is derived by postulating an ocean, throwing in a rock, and calculating the equivalent of the dielectric function of the composite. Then another rock is thrown in and the process repeated. The procedure can be expressed as a differential equation. The solution of this equation is

$$\left(\frac{\varepsilon_b - \varepsilon}{\varepsilon_b - \varepsilon_a}\right)\left(\frac{\varepsilon_a}{\varepsilon}\right)^{q_a} = f_a. \tag{9.37}$$

This model was found to give a good representation of $\varepsilon(\omega)$ of a deposited Rh film, which is polycrystalline with the individual grains completely coated with oxide. Therefore, the oxide is the host material, even though it comprises a small fraction of the total content of the material.

E. Limit theorems; dielectric functions of nanograins.

As can be appreciated, the calculation of an effective-medium expression for a general configuration is a hopeless task. Even if the sizes and shapes of all the grains in the material could be specified, one would still be required to solve the electrostatics problem of the configuration for the internal electric and displacement fields on the scale of the inhomogeneities, then calculate their average values. What is generally done is to assume that one of the existing EMAs provides an adequate description, then hope that the results are not too far removed from reality.

However, limit theorems on two-component composites provide an independent method of assessing the validity of such assumptions, in addition to providing a cross-check on data. We have already mentioned the Wiener limits. Two additional restriction theorems are that of Hashin and Shtrikman, established in 1963 in an elasticity context and valid for any two-phase composite where $f_a$ and $f_b$ are known, and that of Milton and Bergman, published in 1980, for any two-phase composite that in addition is known to be isotropic in either two or three dimensions. The mathematically interesting aspect of these theorems is that, given the dielectric functions of the components of the mixture, all limits can be constructed in the complex $\varepsilon$ plane with a compass and straightedge.

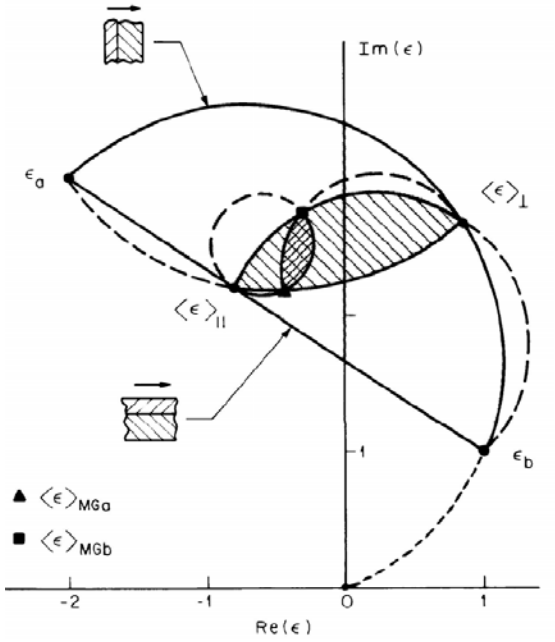


As a basis for discussion, we consider the diagram shown at the right. We assume that we are dealing with two materials, one with a dielectric function $\varepsilon_a = -3 + 3i$ and the other with a dielectric function $\varepsilon_b = 1 + i$. We plot the various limits as a function of the relative volume fractions of the phases *a* and *b*. The outer bounds are the Wiener limits. When no screening is involved, Eq. (9.31) shows that the associated limit is simply a straight line between the end points $\varepsilon_a$ and $\varepsilon_b$, starting at $\varepsilon_a$ for $f_b = 0$ and ending at $\varepsilon_b$ for $f_b = 1$. The maximum-screening limit is also represented by a trajectory starting at $\varepsilon_a$ and ending at $\varepsilon_b$, but this path, given by Eq. (9.33), is a circle. This circular path can be understood from the theory of complex variables: a conformal map in the complex plane converts straight lines ( $f_b$ increasing from 0 to 1 in Eq. (9.33)) to circles and vice versa. However, to draw the circle we need a third point. This is provided by taking the limit $f_b \to \infty$. This is obviously impossible physically, but assuming that we're mathematicians, the calculation is trivial and we find that in this limit $\varepsilon = 0$. We therefore have our third point, and can draw the circle. The result is shown in the diagram.

The larger cross-hatched region represents the Hashin-Shtrikman limits, which are the boundaries if the volume fractions of the two constituents are known. In this example we assume that $f_a = 0.6$ and $f_b = 0.4$. With this information we can locate appropriate points on each of the two Wiener limits. Hashin and Shtrikman showed that with this additional knowledge, the allowed range of $\varepsilon$ was limited to the region bounded by two more circles, one formed by constructing the arc through these two points and $\varepsilon_a$, and the other through these two points and $\varepsilon_b$. The resulting arcs are shown. These correspond mathematically to evaluating $\varepsilon$ in the Garnett EMA for the specific volume fractions of the two materials over the full range of the depolarization parameter *p*, assuming first that the material *a* is contained in the host material *b*, and vice versa. It is seen that these are considerably more restrictive than the Wiener limits.

The last presently known constraint was derived independently by Bergman and Milton in 1980, and consists of the smaller crosshatched region. The Bergman-Milton limits apply if the volume fractions are known and the composite is also known to be isotropic in two or three dimensions. The case where the composite is isotropic in all three dimensions is shown. Here, the defining arcs pass through the appropriate compositional points on the Wiener limits, and the points on the Hashin-Shrikman arcs for $p = 2$.

Throughout, we have assumed that the dielectric functions of the individual grains are in fact the same as those of the same materials in bulk single-crystal form. This assumption is not necessarily valid. Several examples could be mentioned. The figure shows measured dielectric-function $\varepsilon_2$ data for amorphous Si deposited at the different temperatures and rates. The spectral lineshapes for the higher deposition rate are the same, but the amplitude of $\varepsilon_2$ is larger for the higher temperature. From our knowledge that the dielectric function is proportional to the density of induced dipoles, we conclude immediately that the differences here are due to the increase in the packing fraction of the relevant species, the Si-Si bond, and the reduction of empty space (voids) in the material. There is no long-range order, so only a single broad peak appears.

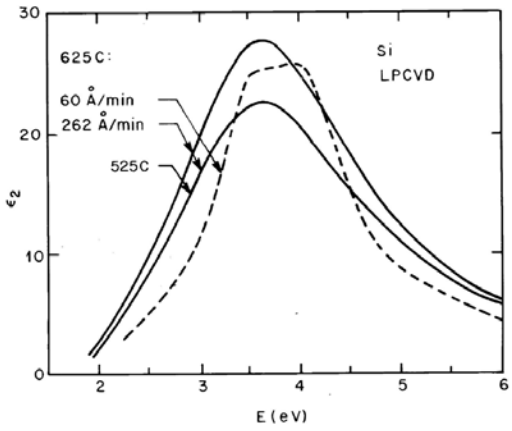


Now consider what happens at the deposition temperature of 625 °C when the deposition rate is reduced. At the slower deposition rate the atoms have more time to reach their preferred crystallographically preferred positions, and the material shows signs of long-range order. However, this spectrum is still very different from that of single-crystal Si, which illustrates a third point: the assumption that the dielectric response of nanograins is the same as that of bulk material needs to be treated with care. Sizes need to become considerably larger that the few nm characteristic of the slow-deposition data in the figure.

In metals, the effect of reduced size appears as increased scattering or equivalently a increased broadening parameter or decreased lifetime, which means a broadening of all spectral features. We have already seen this above with respect to Au. Given an intrinsic lifetime $\tau$, a Fermi velocity $v_F$, and a particle radius *R*, the relation connecting all three is approximately

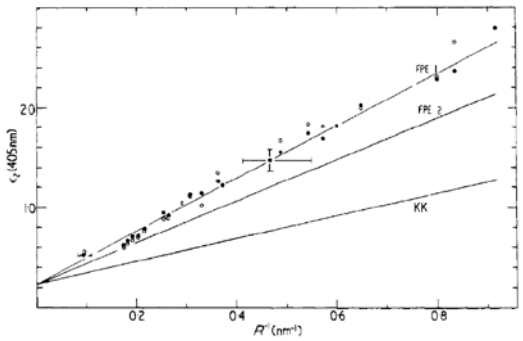


$$\frac{1}{\tau} = \frac{1}{\tau_o} + \frac{v_F}{R} \tag{9.38}$$

where $\tau_o$ is the intrinsic lifetime. Data from Kreibig illustrating this effect in Ag are shown in the figure. One can see that the reciprocal relation is accurately linear over the range of particle sizes covered.

F. Interface plasmons.

We now consider interface plasmons, two-dimensional excitations that have recently received much attention. A thorough discussion requires establishing some background in reflectance, but the topic is included here for completeness.

As noted above, a good way to find plasmons is to set denominators equal to zero. Poles in response functions are physically equivalent to obtaining an output for no input, since $0/0$ is an arbitrary (and not necessarily zero) number. We consider specifically the reflectance of TM-polarized light (p-polarized in older terminology) in the two-phase (substrate/ambient) model. The field reflectance is given by

$$r_p = \frac{\varepsilon_s n_{a\perp} - \varepsilon_a n_{s\perp}}{\varepsilon_s n_{a\perp} + \varepsilon_a n_{s\perp}}. \tag{9.39}$$

where

$$n_{j\perp} = \sqrt{\varepsilon_j - \varepsilon_a \sin^2\theta}\,. \tag{9.40}$$

For future reference, the quantity $n_{j\perp} = ck_{j\perp}/\omega$ is proportional to the component of the wave vector perpendicular to the surface. The complete wave vector must satisfy the dispersion relation

$$c^2k^2/\omega^2 = c^2(k_\parallel^2 + k_\perp^2)/\omega^2 = \varepsilon \tag{9.41}$$

in each medium. This will be discussed in more detail when we cover propagation, but it needs to be introduced here. If the statement about looking for infinities in the overall response is correct, then we should be able to find plasmons by setting $\varepsilon_s n_{a\perp} + \varepsilon_a n_{s\perp} = 0$.

However, the *same* expression with a minus sign instead of a plus sign appears in the numerator, and setting this equal to zero gives Brewster's angle. Let's look at the

Brewster-angle case first. The derivation goes as follows. First we place one term on each side of the equals sign

$$\varepsilon_s n_{a\perp} = \varepsilon_a n_{s\perp} \tag{9.42}$$

then square the above equation to obtain

$$\varepsilon_s^2 \varepsilon_a \cos^2\theta = \varepsilon_a^2(\varepsilon_s - \varepsilon_a \sin^2\theta\,. \tag{9.43}$$

From this we find

$$\varepsilon_s^2(\varepsilon_s - \varepsilon_a) = (\varepsilon_s^2 - \varepsilon_a^2)\sin^2\theta\,. \tag{9.44}$$

Cancelling a common factor gives

$$\sin^2\theta = \frac{\varepsilon_s}{\varepsilon_s + \varepsilon_a} \tag{9.45}$$

so evidently

$$\cos^2\theta = \frac{\varepsilon_a}{\varepsilon_s + \varepsilon_a}\,. \tag{9.46}$$

and we have finally $\tan\theta_B = n_s / n_a$, which is the relation defining Brewster's angle $\theta_B$. As you can see, the derivation is nominally straightforward.

Now let's consider the situation for the positive sign. The first equation changes to

$$\varepsilon_s n_{a\perp} = -\varepsilon_a n_{s\perp}\,. \tag{9.47}$$

We square this relation, and then realize that we're looking at exactly the same equation as before. Yet something must be different, and our challenge is to determine what it is. Going back to the above equation, we see that it could be satisfied if $\varepsilon_s$ is negative. However, this leads to what appears to be a potential difficulty: $n_{s\perp} = \sqrt{\varepsilon_s - \varepsilon_a \sin^2\theta}$ is imaginary. However, this won't be a problem if we can make $n_{a\perp}$ imaginary as well. From our Brewster-angle solution, the equation for $n_{a\perp}$ is

$$n_{a\perp} = n_a \cos\theta = n_a\sqrt{\frac{\varepsilon_a}{\varepsilon_s + \varepsilon_a}}\,. \tag{9.48}$$

This says that all that is required to make $n_{a\perp}$ imaginary is to require that $\varepsilon_s < -\varepsilon_a$. This is therefore the key to the solution – we must expand our view of the allowed values of $\varepsilon_s$. We note that there is no sign ambiguity on taking the square roots to obtain the imaginary *n*, since *n* must always be in the first quadrant of the complex plane.

But what does an imaginary *n* mean? We recall that $k_{a\perp} = (\omega/c)n_{a\perp}$, and that the dispersion equation requires

$$\frac{c^2}{\omega^2}(k_{\|s}^2 + k_{\perp s}^2) = \varepsilon_s\,;\;\; \frac{c^2}{\omega^2}(k_{\|a}^2 + k_{\perp a}^2) = \varepsilon_a\,. \tag{9.49}$$

If we substitute the above solution to find $k_{\|s}$ and $k_{\|a}$, we obtain

$$k_{\|s} = k_{\|a} = \frac{\omega}{c}\sqrt{\frac{\varepsilon_s \varepsilon_a}{\varepsilon_s + \varepsilon_a}}\,. \tag{9.50}$$

These are equal to each other, and real. Of course, the projections of the wave vector on the interface must be equal if the boundary conditions are to be satisfied. Because the solutions are plane waves $e^{i\vec{k}\cdot\vec{r}}$, it now follows that the solution for the vanishing denominator (the plasmon) corresponds to a solution that attenuates exponentially on both sides of the interface but propagates along the interface with a wave vector $k_{\|s} = k_{\|a}$ as given above.

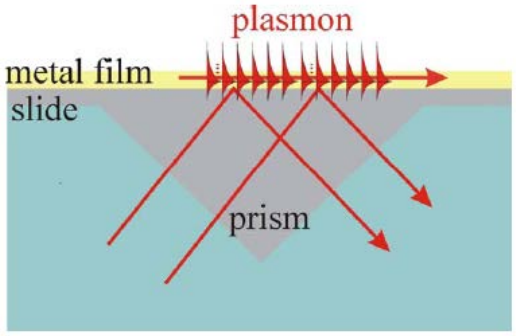


To generate a surface plasmon with an optical beam, it is necessary to match the wave vector of the incident light to the component of the wave vector of the plasmon in the interface plane. For an air interface this is impossible because the interface component of the wave vector of the plasmon is larger than the entire *k* vector in air. However, if we cheat and illuminate the interface using a prism with sufficiently large refractive index, as shown in the diagram at the right, then we can increase the projection of the component of the incident wave vector parallel to the interface, and hence excite the plasmon. By changing the angle of incidence we change the projection angle, and hence change the condition for $\varepsilon(\omega)$, and therefore the frequency $\omega$ at which the plasmon occurs. This is another example of dispersion.

An interesting demonstration of plasmons in thin conducting films was reported by Rhodes et al. (J. Appl. Phys. 103, 093108 (2008)). In this work the TM reflectances of indium tin oxide (ITO) films deposited on a BK7 glass prism were measured for various thicknesses as a function of photon energy and angle of incidence. The results are shown below. The different curves in each panel represent different angles of incidence, starting from 42° (orange) and ending with 53° (purple). The thinnest film, on the top left panel, shows a plasmonic structure at about 1.0 eV. This is itself an interesting case. If we expand the Airy equation for p-polarized light in the three-phase (substrate\overlayer\ambient) model, discussed in Ch. 16, to first order in $d/\lambda$, we find

$$r_p' = r_{po} + \frac{4\pi i d n_a \cos\theta}{\lambda}\,\frac{\varepsilon_s - \varepsilon_o}{\varepsilon_s + \varepsilon_o}\,\frac{\varepsilon_s\varepsilon_o - (\varepsilon_s + \varepsilon_o)\varepsilon_a \sin^2\theta}{\varepsilon_s\varepsilon_a - (\varepsilon_s + \varepsilon_a)\varepsilon_a \sin^2\theta}\,\frac{\varepsilon_a}{\varepsilon_o}\,. \tag{9.51}$$

The interesting term is the last factor. It diverges if $\varepsilon_o \to 0$. The carrier concentration of the ITO film is large enough so the Drude free-electron term added to the background dielectric function arising from transitions at higher energy crosses zero at this point. Thus in the 30 nm film the structure is due to the bulk plasmon. This is exactly the case that we discussed when we introduced the topic of effective-medium theory with respect

to laminar films. It is confirmed because the energy of the bulk plasmon shows no dependence on the angle of incidence of the exciting radiation.

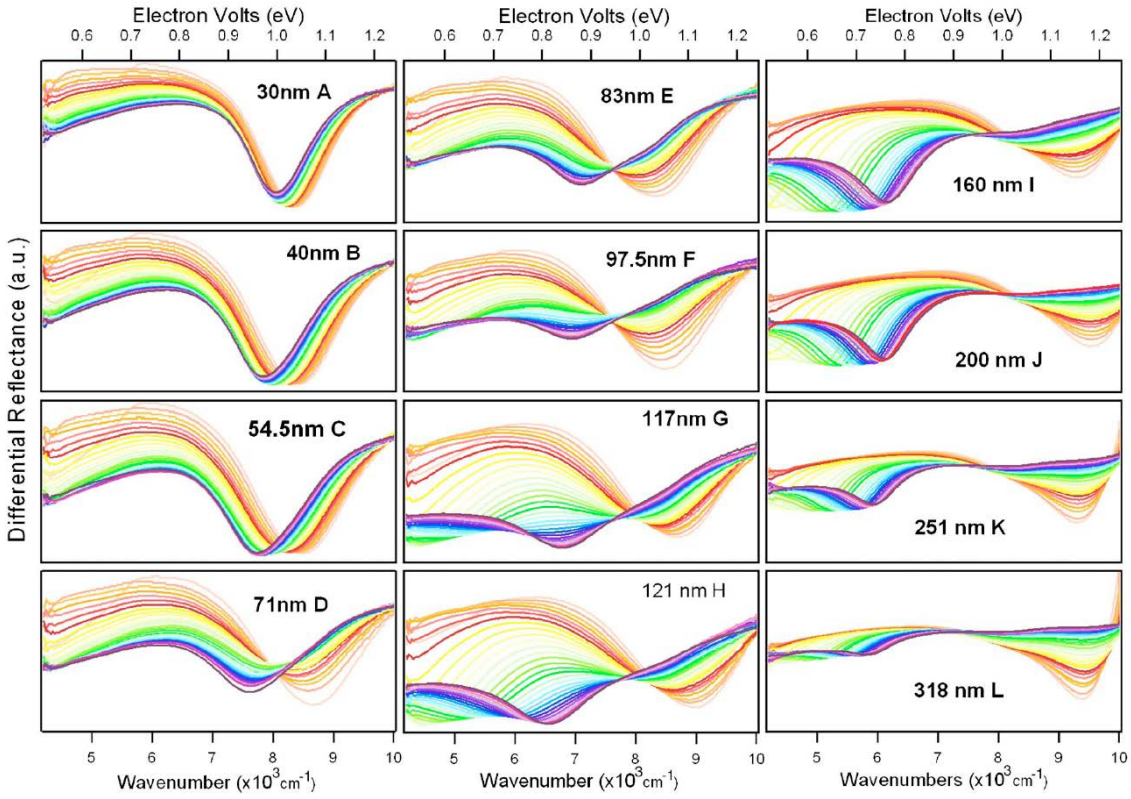


As the thickness is increased, a point is reached where retardation effects become important, so the simple electrostatic theory is no longer valid. The bulk plasmon gradually fades away, but a new structure, the interface plasmon discussed above, begins to emerge. It is first seen at a thickness of 87 nm. By 117 nm the bulk plasmon has disappeared completely, and the new structure is the only one remaining. The proof of its identity is the observed dependence of its energy on the angle of incidence.